A&A 370, L35–L38 (2001)
DOI: 10.1051/0004-6361:20010331

Astronomy & Astrophysics

Letter to the Editor

Dynamical effects of comet P/Halley gas production

K. Szegö[1], J. F. Crifo[2], L. Földy[1], J. S. V. Lagerros[3], and A. V. Rodionov[4]

[1] KFKI Research Institute for Particle and Nuclear Physics, PO Box 49, 1525 Budapest, Hungary
[2] Service d'Aéronomie du CNRS, BP 3, 91371 Verrières le Buisson Cedex, France
[3] Institute for Astronomy and Space Physics, Box 515, 752 37 Uppsala, Sweden
[4] Central Research Institute on Machine Building (TsNIIMASCH), Pionyerskaya St., 4 Korolev, Moscow Region 141070, Russia

Received 12 February 2001 / Accepted 7 March 2001

Abstract. We revisit the rotation of P/Halley taking into account the most essential observational constraints, as well as the external torques affecting the nucleus, in particular the outgassing torque. We solve the dirty ice sublimation equations at each point of the sunlit surface, using, for the first time, the surface shape derived from the 1986 flybys imaging data. We assume that the nuclear surface is homogeneous in composition, thus reducing the number of model free parameters to one only: the dust-to-ice ratio on the surface. Our derived rotation model is a short-axis mode; it is consistent both with the 1986 nucleus imaging data, with the estimated non gravitational force, and with the observed time variations of the nucleus production rates. The outgassing torque results in a significant variation of the angular momentum vector – for the assumed nucleus density of 0.5 g/cm^3.

Key words. comets: P/Halley – rotation mode – data analysis

1. Introduction

The rotation of comet P/Halley has been a matter of debate since its last apparition in 1986. Different data sets and methods of analysis have led to the derivation of conflicting modes of rotation, with conflicting dominant periods, one centred around 2.2 d, the other around 7.4 d or its harmonics, see e.g. Julian (1990, 2000) and references therein. These discrepancies have never been resolved; the authors of the different publications simply dismissed observational evidences that did not support their views. Even though the shape of the nucleus and the orientation of its long axis were derived quite precisely from the images taken during the encounter of the VEGA-1 space probe with comet Halley, these constraints were neglected in many works dedicated to the nucleus rotation. Similarly, it was not investigated whether the postulated nucleus activity is in agreement with the near-nucleus dust patterns observed during the flybys. Finally, the effect of the torque due to the outgassing of the nucleus and to the solar tide were seldom considered. In this brief report we revisit the rotation of the nucleus of comet P/Halley based on the approach of Crifo (1997) and Rodionov et al. (2001), which takes into account these effects self-consistently.

Send offprint requests to: K. Szegö,
e-mail: szego@rmki.kfki.hu

2. Nucleus rotation model

We solve numerically the equations of motion of P/Halley's nucleus, taken to be an asymmetric rigid top, and taking into account the torque due to the gas rocket forces (Rodionov et al. 2001), and the solar tidal torque (Schutz 1981). To compute the value of the torque due to outgassing, we solve the dirty ice sublimation equations at each point of the sunlit surface, with the assumption that the icy area fraction, that is the ratio between the dust and ice on the surface, is everywhere $f = 0.6$ (Crifo 1997). This assumption that the nuclear surface is homogeneous is consistent with that of internal homogeneity done when computing the nucleus inertia. Furthermore, as reported in Rodionov et al. (2001), it has proven successful in accounting quantitatively for the positions of the dust "jets" seen in Halley's coma by the Giotto and VEGA cameras: these "jets" are found to be in fact the consequences of topography-induced azimuthal gas density gradients. Our model also yields the water production rates in a self consistent manner. The assumption that the nucleus is rigid has no effect on our results, because it has been shown that the damping of the rotation due to non-rigidity goes on a time scale of 10^6 years (Harris 1994).

We use the nucleus shape model derived by Merenyi et al. (1990) to calculate the nucleus inertia and torque. This nucleus model is based on the 63 images obtained during the closest portion of the VEGA-1 flyby; their most

important parameters are listed in Szegö et al. (1995). The one-pixel resolution on the images varies between 90×130 m to 450×650 m. Realistically, however, a two-pixel resolution must be used, taking into account uncertainties due to dust contamination; accordingly, the size determination is not more accurate than 0.5 km. The three-dimensional nucleus model derived has the following major characteristics: the overall dimensions are 7.2 km, 7.22 km, 15.3 km, its volume is 365 km^3, the ratios of the inertial momenta are 3.4:3.3:1 assuming a homogeneous mass distribution inside. The longest inertial axis is slightly inclined to the geometrical axis of the body, 3.3° in latitude and 1.1° in longitude, but this deviation is within the limit of the accuracy of the model. For its mass, assuming about 0.5 g/cm^3 density, we take $1.8\,10^{14}$ kg, hence the magnitude of the inertial momenta I_i are of the order of 10^{21} kg m^2. The torque $\boldsymbol{T}$ is a function of the position of the subsolar point, its magnitude is of the order of $5\,10^9$ kg m^2 s^{-2}.

In our analysis of the rotation we use a cometocentric ecliptic coordinate system: its x–y plane is parallel to the ecliptic plane, its x-axis is parallel to the vernal equinox line, and its z-axis points to the ecliptic north. The angles l and b are the longitude and latitude angles, respectively; l is measured in the ecliptic plane, from the x-axis counterclockwise; b is measured from the ecliptic plane. We define a third angle, the roll, denoted by r, as the rotation angle around the l, b direction. We have solved Eqs. (1) and (2) that govern the rotation of an asymmetric top (Landau & Lifshitz 1976). The first set of Eq. (1) is written in the body frame system of reference of the nucleus (ISN) in which the unit vectors $\boldsymbol{e}_i$ of the inertial system are oriented along the axes of the inertial ellipsoid in such a way that $\boldsymbol{e}_1$ is along the direction of smallest inertia momentum and $\boldsymbol{e}_3$ along that of largest; $\boldsymbol{e}_1$ points towards the "bigger end" of the nucleus. The second set of Eqs. (2) describes the motion of the inertial triad (i.e. the set of the $\boldsymbol{e}_i$ vectors) in the cometocentric ecliptic system of reference (CES):

$$\frac{\mathrm{d}\boldsymbol{J}}{\mathrm{d}t} + \boldsymbol{\Omega} \times \boldsymbol{J} = \boldsymbol{T} \tag{1}$$

$$\frac{\mathrm{d}}{\mathrm{d}t}\boldsymbol{e}_i = \boldsymbol{\Omega} \times \boldsymbol{e}_i, \tag{2}$$

where $\boldsymbol{J} \equiv (I_i \Omega_i)$ is the angular momentum vector, and $\boldsymbol{\Omega}$ is the angular velocity vector.

The outgassing torque $\boldsymbol{T}$ acting on the nucleus is defined by:

$$\boldsymbol{T} = -\iint \left(p + \frac{\mathrm{d}M}{\mathrm{d}t} V\right) \boldsymbol{r} \times \boldsymbol{n}\, \mathrm{d}A \tag{3}$$

where p, $\mathrm{d}M/\mathrm{d}t$ and V are the static pressure, mass loss rate and initial exhaust velocity of H_2O at the point $\boldsymbol{r}$ of the surface, respectively, $\boldsymbol{n}$ the unit vector normal to the surface, and $\mathrm{d}A$ the elementary area. The torque clearly depends on the projected position of the Sun on the surface of the nucleus, characterised by the geographic longitude and latitude angles $\phi_\odot(t), \theta_\odot(t)$ defined in the ISN, and upon the heliocentric distance r_h. In practice, in the inner solar system, one can write with excellent accuracy that:

$$\boldsymbol{T}(\phi_\odot, \theta_\odot, r_\mathrm{h}) = \boldsymbol{T}_1(\phi_\odot, \theta_\odot)/r_\mathrm{h}^2 \tag{4}$$

where $\boldsymbol{T}_1$ is the torque computed at 1 AU. The angles $\phi_\odot(t), \theta_\odot(t)$ are computed at each time from the direction of the Sun in the CES and the vectors $\boldsymbol{e}_i$ at that time. The solar tidal torque is evaluated as given in Schutz (1981), actually in that portion of the orbit we consider here, the effect of solar tide is smaller by one order of magnitude than the outgassing torque.

Equation (2) can be written in a simpler form using the fact that $[\boldsymbol{e}_1,\ \boldsymbol{e}_2,\ \boldsymbol{e}_3]$ form an orthonormal system, that is only 3 variables are independent; these can be conveniently the b, l, r angular parameters described above. However, the numerical solution appears to be more stable if Eq. (2) is integrated directly for all nine components of $[\boldsymbol{e}_i]$, making sure at the same time that the system remains orthonormal.

It would have been easy to solve these equations had we had appropriate initial conditions ($[\boldsymbol{e}_i]$ or b, l, r). Instead we used as constraints the orientations of the nucleus long axis as derived from the flyby images (Sagdeev et al. 1989); and we tried different initial conditions $\boldsymbol{\Omega}$ for a 20 days long period starting on March 4.34, 1986, centred close to the Vega 2 encounter; we varied the ratios of the inertial momenta as well. To illustrate this, for the initial value $\boldsymbol{\Omega} = (-0.5,\ -0.2,\ -2.8)$ and inertial ratios (1:3.4:3.5) the l, b, r values obtained for the VEGA 1 and Giotto encounters were (78.3, 16.1, 0.9) and (275.6, −13.6, 28.4), respectively; whereas for $\boldsymbol{\Omega} = (-.44,\ -0.3,\ -2.8)$ and inertia ratios (1.3:2.7:2.83) we got for l, b, r (79.7, 14.0, −1.6) and (272.7, −15.6, 15.3), respectively. We selected the second one, the best approximation to the imaging data. All solutions were short-axis mode rotations; the rotation period about the short axis was very stable, about 1% variation could be seen during one period. The change in the periodicity of b and r was larger, about 10% during one period. In the magnitude of the production rate these variations caused not more than 5% changes, and the variation of the initial conditions did not have sizeable effects on the results presented below.

3. Implications of the rotation model

The variation of the angular momentum vector in the cometocentric ecliptic coordinate system is shown in Fig. 1. The first important conclusion is that the torque has a significant effect on the motion. The magnitude of the angular momentum changes in 20 days by about 0.5%, its direction in l changes from about 28° to 24.5°, in b from −62.9° to −62.2°. These variations are of the same order as those reported in Julian (1990), with the important difference that in previous publications this effect was attributed to gas jets placed arbitrarily on the surface, whereas in our approach this is the effect of the deterministically computed gas emission. It follows from the rate

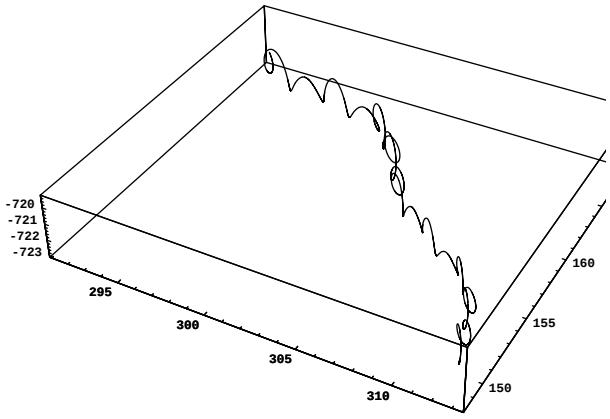

Fig. 1. Variation of the end-point of $\boldsymbol{J}$ in time, the axes are the positions in the ecliptic coordinate system

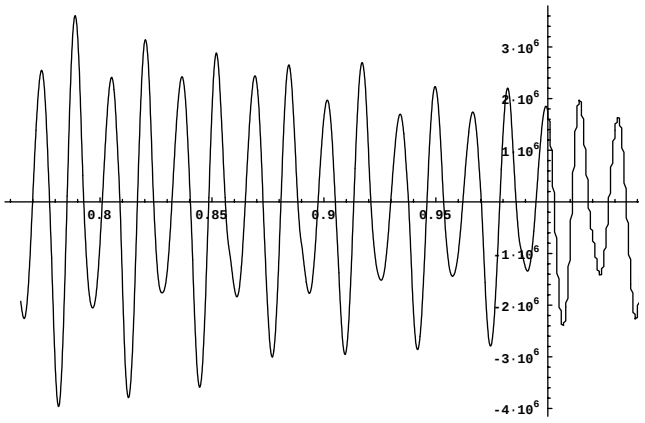

Fig. 2. Non-gravitational force along orbital motion. The horizontal axis shows the heliocentric distance of the nucleus in AU, the vertical axis shows the force in N

of change of the longitudinal component of $\boldsymbol{J}$ that the stability of the spin vector of P/Halley should be considered with certain reservations. The corollary is that the analysis of the rotation of small but active cometary nuclei also require certain care, especially in the case of small but active nuclei such as e.g. comet Wirtanen: in such cases, the rotation can easily be chaotic. In the current calculation the ratio of the average torque to the inertial momenta is about 10^{-11}. As the inertial momenta scales with the size of the nucleus as r^5 and the torque as r^2, this ratio can be huge for a Wirtanen-size comet e.g. on Halley's orbit, and the effects of outgassing must be dominant in setting the rotation mode. This is also true for many other comets as was pointed out by Samarasinha et al. (1996); we shall return to this problem in a separate publication.

To investigate whether our outgassing model is compatible with the non-gravitational perturbations of P/Halley's orbit, we have calculated the non-gravitational forces acting on the nucleus due to this outgassing. This is illustrated in Fig. 2 for the force acting along the orbit (force associated with A_2), the average deceleration/acceleration is $8\,10^4$ N. Taking the above model parameters, this corresponds to $A_2 \quad 0.5\,10^{-9}$ m s^{-2} for this orbital segment. From astronomical observations, calculating A_2 for the whole orbit, Rickman et al. (1987) for P/Halley have derived $A_2 = 0.32\,10^{-8}$ m s^{-2}.

Next, we have investigated whether the computed H_2O production rate is compatible with the production rate observed from ground. In the absence of water production rate data we use other coma species. A compilation of the ground based narrowband photometry data was published by Schleicher et al. (1998) for OH, NH, CN, C_3, C_2 production rates, and for dust using $Af\rho$ values in two spectral intervals. This data set overlaps for a 14 day long period with our calculations. In Fig. 3 we plot these OH, C_2, and dust production rates, normalised to the same average value. Whereas there is a scatter in the numerical values, the major tendencies are similar, the normalised correlations between OH-dust, OH-C_2, and C_2-dust data are 0.78, 0.93, and 0.87, respectively. (We have specifically selected C_2, because Millis & Schleicher 1986, in their famous paper identified a 7.4 d period in the C_2 emission band.) The large scatter in the observed production rates shown in Fig. 4 might be due to the different physical and chemical processes involved in the production of these species; we suspect, however, that the major problem is the use of a time-independent, spherically symmetric, collisionless model (i.e. the Haser model) for data reduction, which introduces large uncertainties in the interpretation. During the time interval we are interested in, the phase angle changed from 56.4° to 66°, this may affect slightly the dust data, but we neglect this in our analysis.

To compare our model with the data, in Fig. 4 we simply overplot the time variation of the calculated water production rate on top of the data shown before. The difficult question how the different species patterns mentioned above are related to the water production pattern is beyond reach in this brief report. Assuming that these patterns are closely similar, let us try to judge the result of Fig. 4. There exist well known statistical methods for such a purpose; their essence is to analyse whether the difference between the model and the measurements follow some well-known statistical distribution. We cannot apply directly these techniques because in our case the measurements are not random in time, and this would introduce a certain bias; and also because time is not a simple model parameter but actually a random variable as well. (This means that the time variable also has an intrinsic uncertainty, since in all data acquisitions – both for the production rates and for the nucleus positions – an unspecified time averaging is involved.)

It is not a trivial question how to define the difference between model values and data; after comparing various techniques we have associated to any data point that model point which is the closest to the given data point in the simple geometrical sense in the plot of Fig. 4. With this association, the normalised correlation between our model and the data for OH, C_2, and the dust components are 0.5, 0.58, and 0.44, respectively. We have checked that modifying the image coordinate scales slightly does not change significantly these correlations.

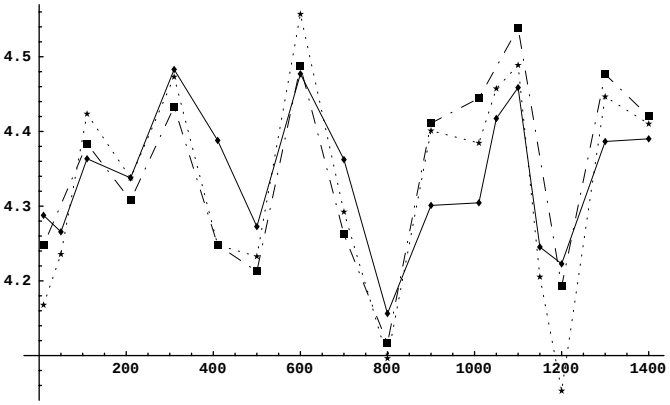

Fig. 3. Logarithms of the production rates derived by Schleicher et al. (1998) normalised arbitrarily: −♦−, dust, −★−, C_2, −■−, OH. The horizontal axis is time in 0.01 d units, starting from 4.34 March, 1986

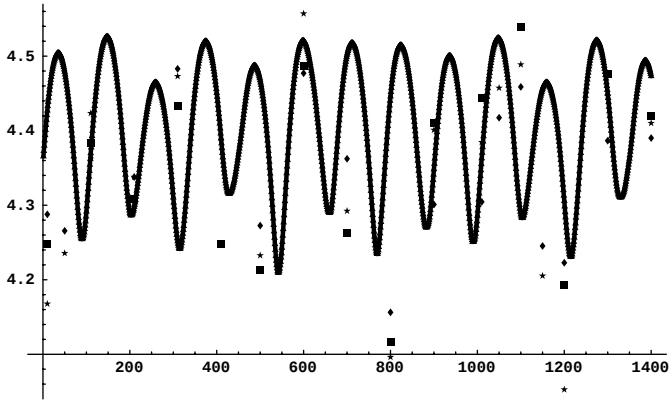

Fig. 4. Comparison between logarithm of the model H_2O production rate (continuous line) and the observations of Fig. 3 (same symbol meanings). The horizontal axis is time in 0.01 d units, starting from 4.34 March, 1986

4. Discussion and conclusions

We have calculated the rotation of P/Halley during a 20 d long period starting on 4.43 March, 1986. The rotational motion was subjected to the essential constraints provided during the flyby missions. The torque and the production rate were calculated in a self-consistent manner. The derived rotation is in agreement with the imaging data obtained during the flyby missions. The production rate of water molecules was found in reasonable agreement with the observed production rate of various coma components, volatiles and dust. We note that the apparent computed 1.1 d period (i.e. one half nucleus rotation quasi-period) of the gas production modulation is close to the period of the ground based observations, and can therefore not be properly revealed by the latter.

Recently Julian et al. (2000) explained the secular behaviour and diurnal amplitude of the observed gas production, assuming five active regions on an ellipsoidal nucleus, and a long-axis mode rotation. Whereas the long-term thermal variation and short term periodic variations are correctly reproduced, we have certain reservations, because a) there are over 20 freely adjustable parameters, b) the location of the active regions differ from those suggested by the 1986 flyby observations (Sagdeev et al. 1987), c) the nucleus shape and orientations during the flybys differ considerably from the observed ones. We think that our model, having only one adjustable parameter – the dust-to-ice surface ratio – and complying with more observational constraints, provides a more satisfactory interpretation of the observations.

The main limitations of the present work are (1) it did not address to the famous cyanogen jets observations of A'Hearn et al. (1986); as the physical source of these structures is unclear to us, we cannot model them yet; (2) while our model has the capability of providing an accurate time-dependent dust emission profile (light curve), the considerable computer resources needed have forced us to delay this achievement to a future phase of our work.

Acknowledgements. Useful discussions with Dr. I. Toth is acknowledged. The work of K. Sz. was supported by the Hungarian OTKA T-32634 grant.

References

A'Hearn, M., Hoban, F. S., Birch, P. V., et al. 1986, Nature, 324, 649
Crifo, J. F. 1997, Icarus, 130, 549
Harris, A. W. 1994, Icarus, 107, 209
Julian, W. H. 1990, Icarus, 88, 355
Julian, W. H., Samarasinha, N. H., & Belton, M. S. J. 2000, Icarus, 144, 160
Landau, L. D., & Lifshitz, E. M. 1976, Mechanics, 3rd edition (Pergamon Press)
Merenyi, E., Foldy, L., Szegö, K., Toth, I., & Kondor, A. 1990, Icarus, 86, 9
Millis, R. L., & Schleicher, D. G. 1986, Nature, 324, 646
Rickman, H., Kamel, L., Festou, M. C., & Froeschle, Cl. 1987, Proc. On the diversity and similarity of comets, ESA SP-278, 471
Rodionov, A. V., Crifo, J. F., Szegö, K., Lagerros, J., & Fulle, M. 2001, A&A, submitted
Sagdeev, R. Z., Smith, B., Szegö, K., et al. 1987, A&A, 187, 835
Sagdeev, R. Z., Szegö, K., Smith, B. A., et al. 1989, AJ, 97, 546
Samarasinha, S. H., Muller, B. E. A., & Belton, J. S. 1996, Planet. Space Sci., 44, 275
Schutz, B. E. 1981, Celestial Mechanics, 24, 173
Schleicher, D. G., Millis, R. L., & Birch, P. V. 1998, Icarus, 132, 397
Szegö, K., Sagdeev, R. Z., Whipple, F. L., et al. 1995, Images Of The Nucleus Of Comet Halley, ed. R. Reinhard, & B. Battrick, ESA SP-1127, vol. 2